ACS APPLIED NANO MATERIALS

www.acsanm.org Article

Modularly Constructed Polyhedral Oligomeric Silsesquioxane-Based Giant Molecules for Unconventional Nanostructure Fabrication

Jing Jiang, Yu Wang, Lun Jin, Chih-Hao Hsu, Shuailin Zhang, Jialin Mao, Wenbin Yin, Tao Li, Bo Ni, Zebin Su, Jiahao Huang, Chrys Wesdemiotis, Kan Yue, Wei Zhang,* and Stephen Z. D. Cheng*

Cite This: *ACS Appl. Nano Mater.* 2020, 3, 2952−2958 Read Online

ACCESS | Metrics & More | Article Recommendations | Supporting Information

ABSTRACT: Controlled assembly of nanoscale building blocks is a promising approach to obtain functional materials with unique properties. Here, we report a way to manipulate the supramolecular structures of giant molecules based on discotic triangle cores and isobutyl polyhedral oligomeric silsesquioxanes (BPOSS) nanoparticles (NPs). It is found that depending upon the number of BPOSS at the periphery of the discotic cores, the packing of these nanoscale components (discotic core and POSS) could be manipulated into either cylindrical or Frank−Kasper (F−K) A15 ($Pm\bar{3}n$) phases. The formation of these supramolecular nanostructures is mandated by the balance between the stacking of the discotic cores and the steric hindrance effect of the BPOSS NPs. This strategy to manipulate the packing of nanoscale building blocks for different supramolecular nanostructures including the fabrication of cylindrical structures and A15 ($Pm\bar{3}n$) phases may be extended to other nanoscale building blocks for future development of materials with complex structures as well as tailored functionalities and properties.

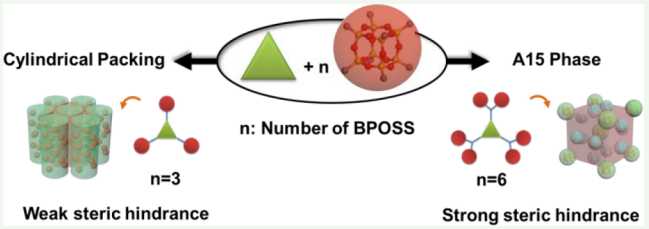

KEYWORDS: *nanoparticles, Frank−Kasper phase, self-assembly, supramolecular chemistry, POSS*

1. INTRODUCTION

Achieving materials with desired properties and functionalities via reverse thinking and designing has been demonstrated as one of the most promising ways in self-assembly ("bottom-up") approaches. In the past two decades, different functionalized nanoscale building blocks have been used to achieve various interesting nanostructures and properties in soft matters.[1−5] Specifically, Frank−Kasper (F−K) phases, which originally appeared in metal-alloys with specifically required spherical motifs,[6,7] are receiving researchers' attention since they have been observed in soft materials, such as supramolecular dendrimers,[8−12] self-organizable dendronized polymers,[13−16] block copolymers,[17−19] surfactants,[20−23] and giant molecules.[24−26] For example, in 1997, the first thermotropic A15 ($Pm\bar{3}n$) phase in soft matter was discovered in dendrimers by Percec et al.[27] Since then, a number of dendrimers were found to assemble into the A15 ($Pm\bar{3}n$) phase,[27−32] σ ($P4_2/mnm$) phase,[33] and quasicrystal phase[34,35] together with the traditional phases, providing a "nanoperiodic table" of supramolecular structures.[10,12,36] Bates et al. discovered the F−K σ ($P4_2/mnm$) phase, C14 ($P6_3/mmc$) phase, and C15 ($Fd\bar{3}$) phase in sphere-forming block copolymer melts.[17−19] Mahanthappa et al. found F−K phases formation in surfactant micelles.[20−23] In the meantime, some simulation and theoretical works about F−K phases have been carried out.[37−46] For example, Kamien et al. investigated the theory of F−K phase formation using a packing model of a hard core and soft corona system.[41,42] Goddard et al. conducted molecular dynamic simulation of supramolecular dendrimer balls on forming A15 ($Pm\bar{3}n$) structures.[37] Glotzer et al. studied the simulation on self-assembly of soft matter, including conventional structures as well as quasicrystals and their approximants.[38−40]

According to those simulations, the building block units must possess specific topological restrictions and secondary interactions. The building blocks in the previously reported examples are mostly soft. Recently, the F−K phases have also been discovered in several categories of giant molecules.[24−26] Giant molecules are a kind of nanoscale macromolecules constructed by the precise molecular nanoparticles (MNPs) as composition units, such as POSS, fullerenes, polyoxometalates, etc.[47−49] The term "giant" is referring to comparison with their small molecular counterparts as the MNP units resemble atoms but are thousands of times larger. Similar concept, such as the nanoelements, have also been used.[12,36] Due to the shape and volume-persistence of the MNPs, the principles of the self-assembly of giant molecules are different from those of the dendrimers or the block copolymers. By rationally

Received: January 27, 2020
Accepted: February 11, 2020
Published: February 11, 2020

https://dx.doi.org/10.1021/acsanm.0c00231
ACS Appl. Nano Mater. 2020, 3, 2952−2958

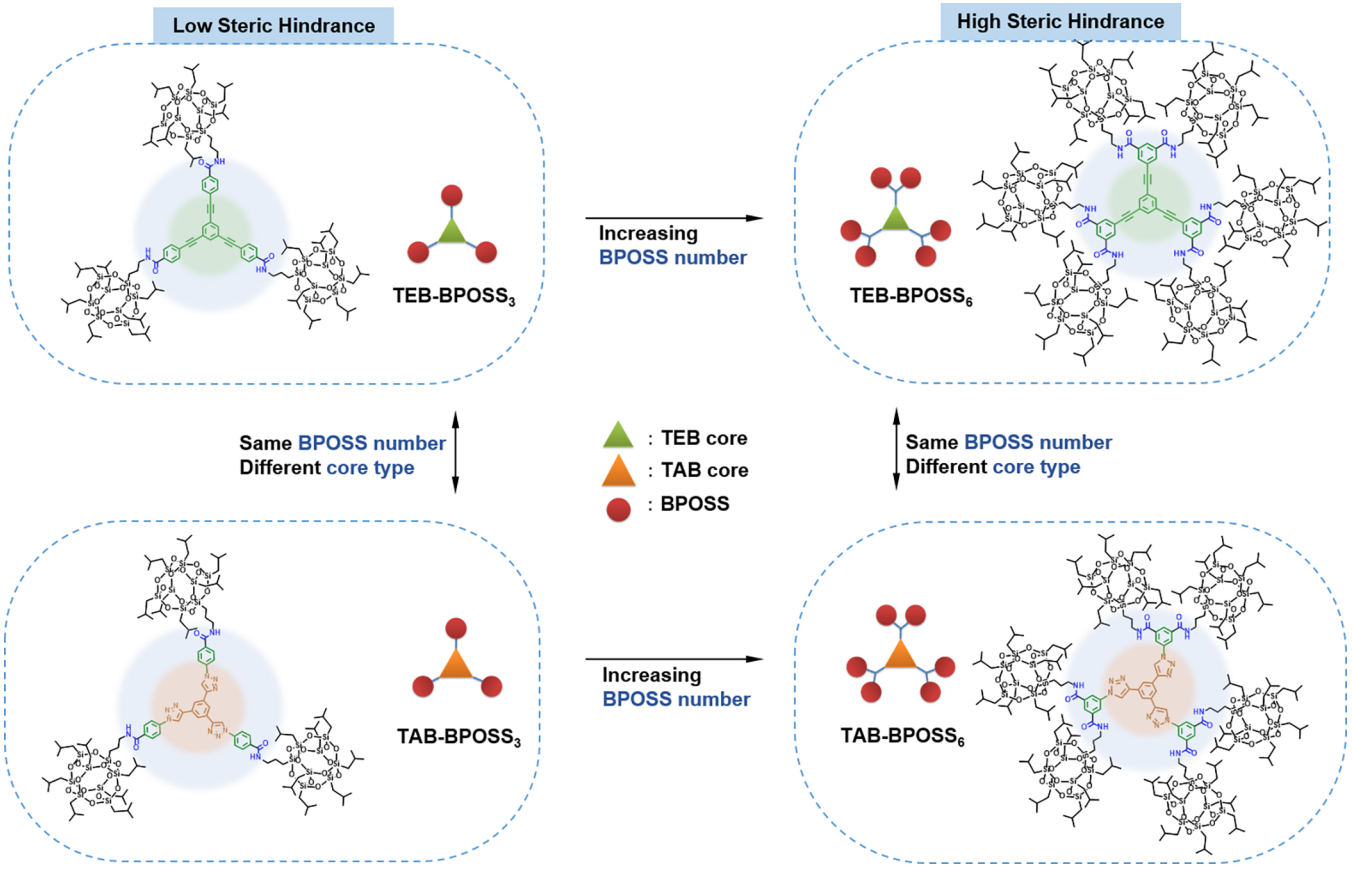

Figure 1. Chemical structures and cartoon illustrations of four giant molecules: **TEB-BPOSS$_3$**, **TEB-BPOSS$_6$**, **TAB-BPOSS$_3$**, and **TAB-BPOSS$_6$**.

molecular design, various supramolecular nanostructures have been achieved,[48,50,51] which are largely influenced by the packing constraints of each individual shape as well as competing interactions.[47] Controlling the packing schemes of these building blocks in a specific combination of composition and topology via a "molecular Lego" approach could result in materials with different structures and properties.[52−54]

Herein, we propose a strategy to manipulate the packing of nanoscale building blocks via specially designed discotic giant molecules to achieve unconventional supramolecular structures. As a proof-of-concept study, two discotic cores were selected to construct the giant molecules: 1,3,5-triethynylbenzene (TEB, simplified as green triangle in Figure 1) and 1,3,5-tritriazole benzene (TAB, orange triangles in the cartoons in Figure 1). Connected with flexible chains, both discotic cores are able to form columnar liquid crystal phases with $\pi-\pi$ stacking distances of 0.3−0.4 nm along the column direction. Those cylindrical assemblies have been widely applied into optoelectronic devices and field effect transistors.[55−57] In this article, three or six relatively rigid and bulky isobutyl POSS (BPOSS) nanoparticles (NPs) (red spheres in the cartoons in Figure 1) are introduced into the periphery of these discotic cores. Since the diameter of BPOSS (1.1−1.2 nm) is much larger than the $\pi-\pi$ stacking distance of the cores (0.3−0.4 nm), therefore, we can directly tune the balance between the steric hindrance of the BPOSS NPs and $\pi-\pi$ interactions of the discotic cores by introducing a different number of rigid BPOSS NPs to the periphery of the discotic cores. When the number of BPOSS is three, the cores may be still able to form columns by rotating the BPOSS NPs around the column. However, when we increase the number of BPOSS to six, the steric hindrance of the BPOSS NPs at periphery could break the columns down, which may deform into spherical motifs and further self-assemble into spherical supramolecular structures (Figure S1).

Different from our previous works, in which the spherical motifs are formed by aggregation of molecules with cone-shape confirmation whose driving force is the immiscibility between hydrophobic and hydrophilic moieties of the giant molecules,[24] in this system, the spherical motifs are formed through breaking down the columns, and the driving forces are the cooperative $\pi-\pi$ interactions and hydrogen bonding competing with the steric hindrance effect. Similar transitions from columnar to spherical phases have been previously observed in dendrimers, which are soft and featured by their generation numbers, molecular tape angle, and solid angle.[29,31,58] Different from the dendrimers, due to the rigidity of the BPOSS NPs, the steric hindrance could be displayed more directly in the giant molecules. As a matter of fact, there are only limited examples shown that discotic molecules with $\pi-\pi$ interactions could also form F−K spherical packings in dendrimers and giant molecules.[26,59−62]

2. EXPERIMENTAL SECTION

2.1. Materials. The giant molecules mentioned in the above text were prepared by the Sonogashira reaction or the CuAAC click reaction. More details on the molecular design and synthesis are provided in the SI Appendix, Section 1.2.

2.2. Sample Preparation. Samples with ordered structures were obtained by thermal annealing at 190−230 °C, followed by rapid quenching. Two sample preparation methods, namely drop-casting and microtoming, were used to process TEM samples. For the drop-

https://dx.doi.org/10.1021/acsanm.0c00231
ACS Appl. Nano Mater. 2020, 3, 2952−2958

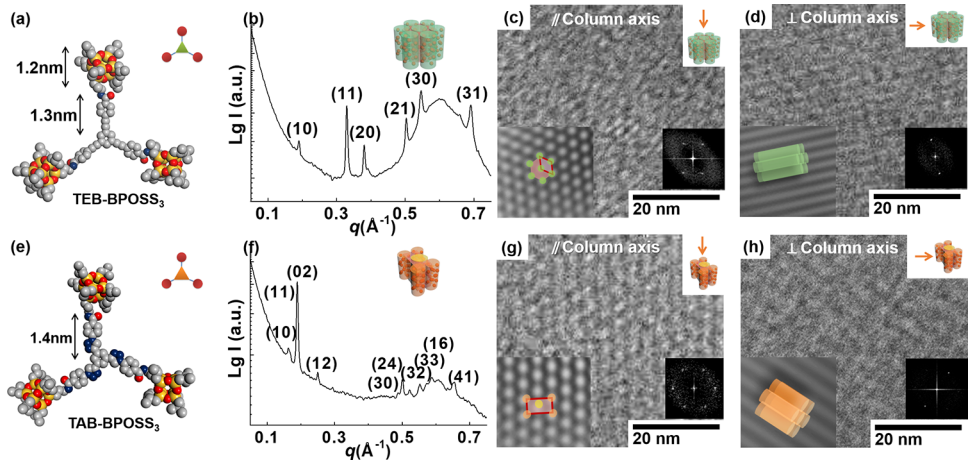

Figure 2. Columnar phases of **TEB-BPOSS$_3$** and **TAB-BPOSS$_3$**. (a) Molecular dimension of **TEB-BPOSS$_3$**. (b) SAXS pattern of **TEB-BPOSS$_3$**. (c,d) Fourier filtered TEM images of **TEB-BPOSS$_3$** taken (c) along and (d) perpendicular to the column axis. Insets: Fourier filtrated TEM images (left bottom) and FFT patterns (right bottom). (e) Molecular dimension of **TAB-BPOSS$_3$**. (f) SAXS pattern of **TAB-BPOSS$_3$**. (g,h) Fourier filtered TEM images of **TAB-BPOSS$_3$** taken (g) along and (h) perpendicular to the column axis. Insets: Fourier filtrated TEM images (left bottom) and FFT patterns (right bottom). The scale bars in the original and Fourier filtered images are the same.

casting method, the sample solution in THF with concentration of 0.5−1.0 mg/mL was dropped onto the carbon-coated copper grids (400 mesh), followed by thermally annealing at corresponding temperature overnight before TEM measurement. For the microtoming method, thin slices of annealed samples for TEM were prepared by utilizing a Leica EM UC7 microtome.

2.3. Characterization. SAXS experiments were performed on a Rigaku MicroMax002+ instrument equipped with a 2D multiwire area detector and a microfocus sealed copper tube. Synchrotron SAXS experiments were conducted at 12-ID-B, C station with X-ray energy of 12 keV at the Advanced Photon Source (APS) of Argonne National Laboratory. Bright field TEM images of the thin-slice samples were collected on a JEOL-1230 TEM with an accelerating voltage of 120 kV and a CCD camera. Fourier filtering of the TEM image was carried out with the reported FFTW implementation method.[24,63] More details on the characterization are provided in the SI Appendix, Section 1.

3. RESULTS AND DISCUSSION

The chemical structures of the four different designed giant molecules are shown in Figure 1. Among them, **TEB-BPOSS$_3$** and **TEB-BPOSS$_6$** possess the same type of core but two different periphery BPOSS numbers (three versus six), and so is the same for **TAB-BPOSS$_3$** and **TAB-BPOSS$_6$**. Their detailed synthetic routes are in the Supporting Information (Schemes S1−S9). Briefly, **TEB-BPOSS$_3$** and **TEB-BPOSS$_6$** are prepared by the Sonogashira coupling of iodo-functionalized BPOSS and alkyne-functionalized 1,3,5-triethynylbenzene cores, while **TAB-BPOSS$_3$** and **TAB-BPOSS$_6$** are synthesized by the copper-catalyzed azide−alkyne cycloaddition (CuAAC) "click" reactions of azo-functionalized BPOSS and alkyne-functionalized 1,3,5-triethynylbenzene cores. The precise chemical structures and monodispersity of these four molecules have been confirmed by ^{1}H and ^{13}C NMR spectra (Figures S2−S9), matrix assisted laser desorption/ionization-time-of-flight (MALDI-TOF) mass spectra (Figure S14a), and gel permeation chromatography (GPC) results (Figure S14b).

All four samples show excellent thermal stability up to 300 °C (Figure S16). Ordered packing can thus be obtained via thermal annealing at 190 °C−230 °C followed by rapid quenching. Prolonging annealing time (e.g., overnight) does not change the formed structures. The small angle X-ray scattering (SAXS) technique is used to monitor the formation of ordered structures in the bulk samples. After thermal treatment at 230 °C for 2 min and subsequent quenching, **TEB-BPOSS$_3$** shows a set of well-resolved SAXS peaks (Figure 2b) with a characteristic scattering vector ratio of $1:\sqrt{3}:2$. These peaks can be assigned to a hexagonal columnar lattice, and the projected 2D hexagonal lattice parameters are determined as $a = b = 3.83$ nm and $\gamma = 120°$. The relatively low intensity of the first diffraction peak (10) here is possibly due to the electron density variation within the supramolecular columns, which could also be supported by simplified atomic simulation (Figure S18). Similar phenomena have been attributed to factors such as the presence of a hollow center, variation of the alkyl chain length, introduction of fluorinated chains, and the polyhedral shape of the doubly segregated aliphatic-aromatic supramolecular structure.[32,64,65]

To further verify this assignment, transmission electron microscopy (TEM) experiments have been carried out for microtomed samples without staining. The scale of the ordered domains are typically several hundreds of nanometers. As shown in Figure 2c, hexagonal columnar packing perpendicular to the column axis can be clearly seen for **TEB-BPOSS$_3$**. The Fourier filtration process is used to enhance the image contrast (see Supporting Information Section 1.1.2 for details). The intercolumn d-spacing is measured as 3.6 ± 0.1 nm, which is in agreement with that from the SAXS data (3.83 nm). In the TEM image, the darker matrix is attributed to the BPOSS NPs, and the light dots are the stacked **TEB** cores. Notably, the measured diameter of the light dot is about 2.4 nm, consistent with the diameter of a **TEB** core (Figure S19). The distance between two light dots is about 1.2 nm, indicating that the BPOSS NPs of adjacent columns may partially interdigitate with each other. TEM images along the [10] direction can also be observed (Figure 2d) with an intercolumn d-spacing of 3.1 ± 0.1 nm, matching well with the (10) d-spacing determined from X-ray data (3.32 nm).

Interestingly, **TAB-BPOSS$_3$** shows a different set of SAXS diffraction peaks with a q-ratio of $\sqrt{3}:\sqrt{4}:\sqrt{7}$ (Figure 2f). These peaks can be assigned as the (10), (11), and (12) planes in a 2D rectangular lattice with lattice parameters of $a = 3.9$

https://dx.doi.org/10.1021/acsanm.0c00231
ACS Appl. Nano Mater. 2020, 3, 2952−2958

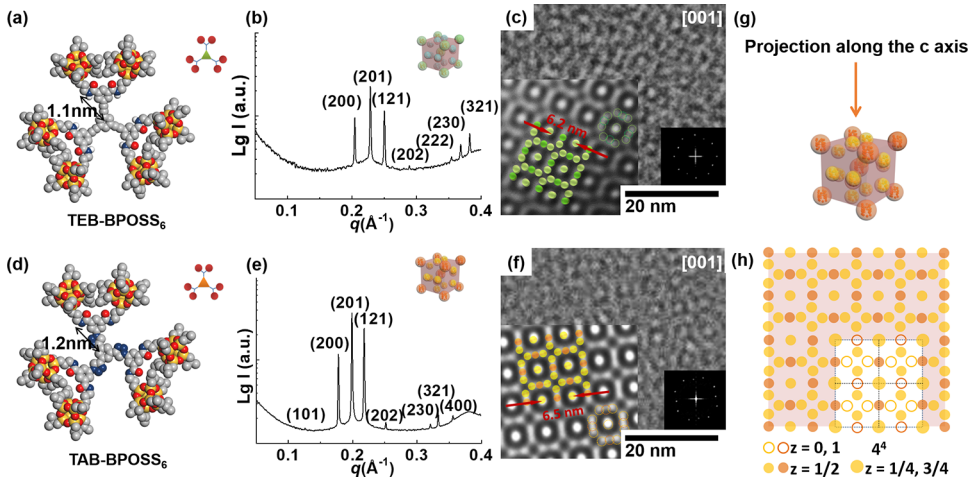

Figure 3. A15 ($Pm\bar{3}n$) phase formation of **TEB-BPOSS$_6$** and **TAB-BPOSS$_6$**. (a) Molecular dimension of **TEB-BPOSS$_6$**. (b) SAXS pattern and (c) Fourier filtrated TEM images of **TEB-BPOSS$_6$**. Insets: Fourier filtrated TEM images (left bottom) and FFT patterns (right bottom). (d) Molecular dimension of **TAB-BPOSS$_6$**. (e) SAXS pattern and (f) Fourier filtered TEM images of **TAB-BPOSS$_6$**. Insets: Fourier filtrated TEM images (left bottom) and FFT patterns (right bottom). (g) Illustration of the A15 ($Pm\bar{3}n$) structure and (h) the 2D 4^4 tiling patterns along the [001] direction. The spheres located at sparse layers (z = 1/4 and 3/4) are represented by large filled circles. The spheres at z = 0 (small open circles) and 1/2 (small filled circles) form the dense nets. The scale bars in the original and Fourier filtered images are the same.

nm, b = 6.64 nm, and γ = 90° and two columns per lattice (for a detailed structure, see Figure S20). This rectangular lattice can also be confirmed by TEM images, as the measured angle of the center column with two neighboring columns deviated from a perfect 60° in a typical hexagonal lattice (Figure 2g). Moreover, lattice parameters determined from this TEM image are a = 3.9 ± 0.1 nm and b = 6.6 ± 0.1 nm, which are in excellent agreement with those obtained from SAXS data. The formation of a rectangular lattice may result from the tilting of the discotic **TAB** cores within the column, which made the cross section of the columns deviate from circular shape and close to an elliptical shape along the column axis.

Changing the number of BPOSS NPs connected to the triangle core from three to six alters the packing scheme and leads to completely different supramolecular nanostructures. **TEB-BPOSS$_6$** and **TAB-BPOSS$_6$** both show SAXS patterns with three major peaks of q-ratios of $\sqrt{4}:\sqrt{5}:\sqrt{6}$ (Figures 3b and 3e), which are characteristic of a 3D F–K A15 ($Pm\bar{3}n$) phase with spherical motifs.[6,7] Those diffraction peaks can be indexed as (200), (201), and (121) of the A15 ($Pm\bar{3}n$) lattice. All the other diffraction peaks can also be clearly indexed as in Figures 3b and 3e. The unit cell parameters are determined as $a = b = c$ = 6.16 nm, $\alpha = \beta = \gamma$ = 90° for **TEB-BPOSS$_6$** and $a = b = c$ = 7.06 nm, $\alpha = \beta = \gamma$ = 90° for **TAB-BPOSS$_6$**, respectively. No sharp diffractions can be observed in their WAXD patterns (Figure S21), indicating that BPOSS NPs are not crystallized. Moreover, TEM images taken along the [001] direction exhibit the characteristic 4^4 tiling patterns for both samples without staining (Figures 3c and 3f–h), confirming the A15 ($Pm\bar{3}n$) structure.[24] The light circles refer to the aromatic cores, and the darker area refers to the BPOSS NPs. Spheres of two sizes are observed in the TEM images, suggesting that the A15 ($Pm\bar{3}n$) structures may be the Cr_3Si type.[66−68] The lattice parameters obtained from TEM images are consistent with those determined from SAXS profiles.

We reason that the changes in the assembled structures from the columns to the A15 ($Pm\bar{3}n$) structure are due to the spatial packing allowed at the periphery of the discotic cores. The discotic cores prefer to stack into columns via $\pi-\pi$ interactions (Figure 4a). The existence of weak $\pi-\pi$ interactions is supported by the WAXD spectra (Figure S21). It should be noted that, in our molecular design, we specifically introduce the amide groups in the linkers, which could generate hydrogen bonding between neighboring molecules and thus further assist the stacking of the discotic cores. The presence of hydrogen bonding can be detected by Fourier transform infrared (FT-IR) spectroscopy (Figure S22). The necessity of this hydrogen bonding in the formation of the structures is illustrated by study on another set of similar molecules with only ester linkages (Schemes S6–S9). The observation that replacing the amide groups by ester linkages completely prevents the formation of ordered structures (Figure S23) highlights the significance of hydrogen bonding for constricting the discotic cores in addition to the weak $\pi-\pi$ interactions.

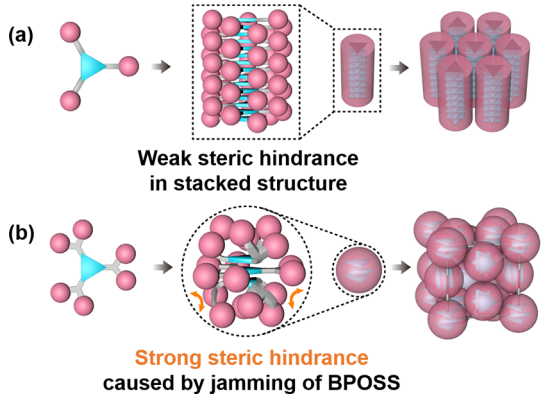

Figure 4. Proposed molecular packing scheme: (a) columnar structure and (b) A15 ($Pm\bar{3}n$) structure. The packing is controlled by the competition between the periphery steric hindrance caused by BPOSS NPs (red spheres) and stacking of the cores (blue triangles).

BPOSS NPs are shape and volume persistent. With only three BPOSS NPs at the periphery of the discotic core (as for **TEB-BPOSS$_3$** and **TAB-BPOSS$_3$**), there is enough space for BPOSS NPs to arrange themselves around the core stem by

https://dx.doi.org/10.1021/acsanm.0c00231
ACS Appl. Nano Mater. 2020, 3, 2952−2958

rotating the molecule along the column direction, so the columnar motifs are retained.[3] However, when the number of BPOSS NPs increases to six per core (as for **TEB-BPOSS$_6$** and **TAB-BPOSS$_6$**), the NPs at the periphery region are too crowded to maintain the columnar structure. The steric hindrance generated by BPOSS NPs plays a counter role to maintaining the columns. As a result, the columns may prefer to periodically break down along the column axis for releasing the steric hindrance (Figure 4b). In order to balance the extra-volume requirement and the interactions among discotic cores, a bowl-shaped deformation may occur as shown in Figure 4b, leading to formation of spherical motifs, which could further self-assemble into the F−K A15 ($Pm\bar{3}n$) phase. A similar mechanism has also been reported in the self-assembly of some dendronized discotic molecules, a different class of molecules, in which their deformation from planar conformation into a bowl shape is induced by the changes in the packing mode of the outer aliphatic region upon temperature increase, leading to the transition from columnar to spherical phases.[59−62,69,70] We would expect that discotic molecules modified with other structural units with persistent shape and volume (e.g., fullerenes) could also assemble in this way. The measured density values of these two A15 ($Pm\bar{3}n$) phases are 1.10 g/cm^3 for both **TEB-BPOSS$_6$** and **TAB-BPOSS$_6$**. Therefore, in each unit cell, it can be calculated that there are about 24 molecules for **TEB-BPOSS$_6$** and 30 molecules for **TAB-BPOSS$_6$**, respectively. Since there are eight motifs in each lattice cell of the A15 ($Pm\bar{3}n$) structure, the average numbers of the molecules in each spherical motif are three to four molecules for **TEB-BPOSS$_6$** and **TAB-BPOSS$_6$** (see Supporting Information Section 3 for details). This result indicates that in these two samples, the column breaking takes place in every three or four molecules along the imaginary columnar stacking.

4. CONCLUSION

In conclusion, a new strategy performed by symmetric giant molecules has been successfully utilized to construct supramolecular nanostructures with different symmetries. Using a nanoscale discotic core and rigid BPOSS NPs as the prototype models, we show that the balance between the stacking of the cores and the steric hindrance of BPOSS plays a critical role in the formation of self-assembled nanostructures, such as cylinders or spherical Frank−Kasper A15 phases. The rigidity of the BPOSS NPs makes the steric hindrance controlled more directly and simply here. The supramolecular motifs can be tuned from cylindrical to spherical by simply increasing the BPOSS number. This strategy is not limited to BPOSS NPs or the triangle cores. Incorporation of other nanoparticles such as fullerenes, polyoxometalates, and proteins with other joint units can further diversify the packing schemes of such nano building blocks, which might provide insights toward the development of functional materials with specific nanostructures and unexpected properties.

■ ASSOCIATED CONTENT

Supporting Information

The Supporting Information is available free of charge at https://pubs.acs.org/doi/10.1021/acsanm.0c00231.

Details of the synthesis, chemical structure characterization, additional results, and analysis (PDF)

■ AUTHOR INFORMATION

Corresponding Authors

Wei Zhang − *Department of Polymer Science, College of Polymer Science and Polymer Engineering, University of Akron, Akron, Ohio 44325-3909, United States;* orcid.org/0000-0002-9321-6411; Email: wz25@zips.uakron.edu

Stephen Z. D. Cheng − *Department of Polymer Science, College of Polymer Science and Polymer Engineering, University of Akron, Akron, Ohio 44325-3909, United States; South China Advanced Institute for Soft Matter Science and Technology, South China University of Technology, Guangzhou 510640, China;* orcid.org/0000-0003-1448-0546; Email: scheng@uakron.edu

Authors

Jing Jiang − *Department of Polymer Science, College of Polymer Science and Polymer Engineering, University of Akron, Akron, Ohio 44325-3909, United States*

Yu Wang − *Department of Polymer Science, College of Polymer Science and Polymer Engineering, University of Akron, Akron, Ohio 44325-3909, United States;* orcid.org/0000-0002-9029-1846

Lun Jin − *Department of Polymer Science, College of Polymer Science and Polymer Engineering, University of Akron, Akron, Ohio 44325-3909, United States*

Chih-Hao Hsu − *Department of Polymer Science, College of Polymer Science and Polymer Engineering, University of Akron, Akron, Ohio 44325-3909, United States*

Shuailin Zhang − *Department of Polymer Science, College of Polymer Science and Polymer Engineering, University of Akron, Akron, Ohio 44325-3909, United States*

Jialin Mao − *Department of Chemistry, University of Akron, Akron, Ohio 44325-3601, United States;* orcid.org/0000-0002-5011-4378

Wenbin Yin − *Department of Polymer Science, College of Polymer Science and Polymer Engineering, University of Akron, Akron, Ohio 44325-3909, United States*

Tao Li − *X-ray Science Division, Advanced Photon Source Argonne National Laboratory, Lemont 60439, United States; Department of Chemistry and Biochemistry, Northern Illinois University, DeKalb, Illinois 60115, United States*

Bo Ni − *Department of Polymer Science, College of Polymer Science and Polymer Engineering, University of Akron, Akron, Ohio 44325-3909, United States*

Zebin Su − *Department of Polymer Science, College of Polymer Science and Polymer Engineering, University of Akron, Akron, Ohio 44325-3909, United States*

Jiahao Huang − *Department of Polymer Science, College of Polymer Science and Polymer Engineering, University of Akron, Akron, Ohio 44325-3909, United States*

Chrys Wesdemiotis − *Department of Polymer Science, College of Polymer Science and Polymer Engineering and Department of Chemistry, University of Akron, Akron, Ohio 44325-3909, United States;* orcid.org/0000-0002-7916-4782

Kan Yue − *South China Advanced Institute for Soft Matter Science and Technology, South China University of Technology, Guangzhou 510640, China*

Complete contact information is available at: https://pubs.acs.org/10.1021/acsanm.0c00231

Notes

The authors declare no competing financial interest.

https://dx.doi.org/10.1021/acsanm.0c00231
ACS Appl. Nano Mater. 2020, 3, 2952−2958

■ ACKNOWLEDGMENTS

This work was financially supported by NSF (DMR-1408872 to S.Z.D.C. and CHE-1808115 to C.W.). This research used resources of the Advanced Photon Source, a U.S. Department of Energy (DOE) Office of Science User Facility operated for the DOE Office of Science by Argonne National Laboratory under Contract No. DE-AC02-06CH11357.

■ REFERENCES

(1) Percec, V.; Wilson, D. A.; Leowanawat, P.; Wilson, C. J.; Hughes, A. D.; Kaucher, M. S.; Hammer, D. A.; Levine, D. H.; Kim, A. J.; Bates, F. S.; Davis, K. P.; Lodge, T. P.; Klein, M. L.; DeVane, R. H.; Aqad, E.; Rosen, B. M.; Argintaru, A. O.; Sienkowska, M. J.; Rissanen, K.; Nummelin, S.; Ropponen, J. Self-Assembly of Janus Dendrimers into Uniform Dendrimersomes and Other Complex Architectures. *Science* **2010**, *328*, 1009−1014.

(2) Mai, Y.; Eisenberg, A. Self-assembly of block copolymers. *Chem. Soc. Rev.* **2012**, *41*, 5969−5985.

(3) Wang, C.-L.; Zhang, W.-B.; Sun, H.-J.; Van Horn, R. M.; Kulkarni, R. R.; Tsai, C.-C.; Hsu, C.-S.; Lotz, B.; Gong, X.; Cheng, S. Z. D. A Supramolecular "Double-Cable" Structure with a 12944 Helix in a Columnar Porphyrin-C60 Dyad and its Application in Polymer Solar Cells. *Adv. Energy Mater.* **2012**, *2*, 1375−1382.

(4) He, X.; Fan, J.; Zou, J.; Wooley, K. L. Reversible photopatterning of soft conductive materials via spatially-defined supramolecular assembly. *Chem. Commun.* **2016**, *52*, 8455−8458.

(5) Laramy, C. R.; O'Brien, M. N.; Mirkin, C. A. Crystal engineering with DNA. *Nat. Rev. Mater.* **2019**, *4*, 201−224.

(6) Frank, F. C.; Kasper, J. S. Complex Alloy Structures Regarded as Sphere Packings. I. Definitions and Basic Principles. *Acta Crystallogr.* **1958**, *11*, 184−190.

(7) Frank, F. C.; Kasper, J. S. Complex alloy structures regarded as sphere packing: 2. Analysis and classfication of representative structures. *Acta Crystallogr.* **1959**, *12*, 483−499.

(8) Percec, V.; Cho, W.-D.; Ungar, G.; Yeardley, D. J. P. Synthesis and Structural Analysis of Two Constitutional Isomeric Libraries of AB2-Based Monodendrons and Supramolecular Dendrimers. *J. Am. Chem. Soc.* **2001**, *123*, 1302−1315.

(9) Percec, V.; Peterca, M.; Sienkowska, M. J.; Ilies, M. A.; Aqad, E.; Smidrkal, J.; Heiney, P. A. Synthesis and Retrostructural Analysis of Libraries of AB3 and Constitutional Isomeric AB2 Phenylpropyl Ether-Based Supramolecular Dendrimers. *J. Am. Chem. Soc.* **2006**, *128*, 3324−3334.

(10) Rosen, B. M.; Wilson, D. A.; Wilson, C. J.; Peterca, M.; Won, B. C.; Huang, C.; Lipski, L. R.; Zeng, X.; Ungar, G.; Heiney, P. A.; Percec, V. Predicting the Structure of Supramolecular Dendrimers via the Analysis of Libraries of AB3 and Constitutional Isomeric AB2 Biphenylpropyl Ether Self-Assembling Dendrons. *J. Am. Chem. Soc.* **2009**, *131*, 17500−17521.

(11) Rosen, B. M.; Wilson, C. J.; Wilson, D. A.; Peterca, M.; Imam, M. R.; Percec, V. Dendron-Mediated Self-Assembly, Disassembly, and Self-Organization of Complex Systems. *Chem. Rev.* **2009**, *109*, 6275−6540.

(12) Rosen, B. M.; Peterca, M.; Huang, C.; Zeng, X.; Ungar, G.; Percec, V. Deconstruction as a Strategy for the Design of Libraries of Self-Assembling Dendrons. *Angew. Chem., Int. Ed.* **2010**, *49*, 7002−7005.

(13) Percec, V.; Ahn, C. H.; Ungar, G.; Yeardley, D. J. P.; Möller, M.; Sheiko, S. S. Controlling polymer shape through the self-assembly of dendritic side-groups. *Nature* **1998**, *391*, 161−164.

(14) Sun, H.-J.; Zhang, S.; Percec, V. From structure to function via complex supramolecular dendrimer systems. *Chem. Soc. Rev.* **2015**, *44*, 3900−3923.

(15) Holerca, M. N.; Sahoo, D.; Peterca, M.; Partridge, B. E.; Heiney, P. A.; Percec, V. A Tetragonal Phase Self-Organized from Unimolecular Spheres Assembled from a Substituted Poly(2-oxazoline). *Macromolecules* **2017**, *50*, 375−385.

(16) Holerca, M. N.; Sahoo, D.; Partridge, B. E.; Peterca, M.; Zeng, X.; Ungar, G.; Percec, V. Dendronized Poly(2-oxazoline) Displays within only Five Monomer Repeat Units Liquid Quasicrystal, A15 and σ Frank−Kasper Phases. *J. Am. Chem. Soc.* **2018**, *140*, 16941−16947.

(17) Lee, S.; Bluemle, M. J.; Bates, F. S. Discovery of a Frank-Kasper σ Phase in Sphere-Forming Block Copolymer Melts. *Science* **2010**, *330*, 349−353.

(18) Lee, S.; Leighton, C.; Bates, F. S. Sphericity and symmetry breaking in the formation of Frank−Kasper phases from one component materials. *Proc. Natl. Acad. Sci. U. S. A.* **2014**, *111*, 17723−17731.

(19) Kim, K.; Schulze, M. W.; Arora, A.; Lewis, R. M.; Hillmyer, M. A.; Dorfman, K. D.; Bates, F. S. Thermal processing of diblock copolymer melts mimics metallurgy. *Science* **2017**, *356*, 520−523.

(20) Perroni, D. V.; Mahanthappa, M. K. Inverse Pm$\bar{3}$n cubic micellar lyotropic phases from zwitterionic triazolium gemini surfactants. *Soft Matter* **2013**, *9*, 7919−7922.

(21) Baez-Cotto, C. M.; Mahanthappa, M. K. Micellar Mimicry of Intermetallic C14 and C15 Laves Phases by Aqueous Lyotropic Self-Assembly. *ACS Nano* **2018**, *12*, 3226−3234.

(22) Jayaraman, A.; Mahanthappa, M. K. Counterion-Dependent Access to Low-Symmetry Lyotropic Sphere Packings of Ionic Surfactant Micelles. *Langmuir* **2018**, *34*, 2290−2301.

(23) Jayaraman, A.; Zhang, D. Y.; Dewing, B. L.; Mahanthappa, M. K. Path-Dependent Preparation of Complex Micelle Packings of a Hydrated Diblock Oligomer. *ACS Cent. Sci.* **2019**, *5*, 619−628.

(24) Huang, M.; Hsu, C.-H.; Wang, J.; Mei, S.; Dong, X.; Li, Y.; Li, M.; Liu, H.; Zhang, W.; Aida, T.; Zhang, W.-B.; Yue, K.; Cheng, S. Z. D. Selective assemblies of giant tetrahedra via precisely controlled positional interactions. *Science* **2015**, *348*, 424−428.

(25) Yue, K.; Huang, M.; Marson, R. L.; He, J.; Huang, J.; Zhou, Z.; Wang, J.; Liu, C.; Yan, X.; Wu, K.; Guo, Z.; Liu, H.; Zhang, W.; Ni, P.; Wesdemiotis, C.; Zhang, W.-B.; Glotzer, S. C.; Cheng, S. Z. D. Geometry induced sequence of nanoscale Frank−Kasper and quasicrystal mesophases in giant surfactants. *Proc. Natl. Acad. Sci. U. S. A.* **2016**, *113*, 14195−14200.

(26) Su, Z.; Hsu, C.-H.; Gong, Z.; Feng, X.; Huang, J.; Zhang, R.; Wang, Y.; Mao, J.; Wesdemiotis, C.; Li, T.; Seifert, S.; Zhang, W.; Aida, T.; Huang, M.; Cheng, S. Z. D. Identification of a Frank−Kasper Z phase from shape amphiphile self-assembly. *Nat. Chem.* **2019**, *11*, 899−905.

(27) Balagurusamy, V. S. K.; Ungar, G.; Percec, V.; Johansson, G. Rational Design of the First Spherical Supramolecular Dendrimers Self-Organized in a Novel Thermotropic Cubic Liquid-Crystalline Phase and the Determination of Their Shape by X-ray Analysis. *J. Am. Chem. Soc.* **1997**, *119*, 1539−1555.

(28) Hudson, S. D.; Jung, H. T.; Percec, V.; Cho, W. D.; Johansson, G.; Ungar, G.; Balagurusamy, V. S. K. Direct Visualization of Individual Cylindrical and Spherical Supramolecular Dendrimers. *Science* **1997**, *278*, 449−452.

(29) Percec, V.; Cho, W. D.; Mosier, P. E.; Ungar, G.; Yeardley, D. J. P. Structural Analysis of Cylindrical and Spherical Supramolecular Dendrimers Quantifies the Concept of Monodendron Shape Control by Generation Number. *J. Am. Chem. Soc.* **1998**, *120*, 11061−11070.

(30) Percec, V.; Cho, W.-D.; Möller, M.; Prokhorova, S. A.; Ungar, G.; Yeardley, D. J. P. Design and Structural Analysis of the First Spherical Monodendron Self-Organizable in a Cubic Lattice. *J. Am. Chem. Soc.* **2000**, *122*, 4249−4250.

(31) Ungar, G.; Percec, V.; Holerca, M. N.; Johansson, G.; Heck, J. A. Heat-Shrinking Spherical and Columnar Supramolecular Dendrimers: Their Interconversion and Dependence of Their Shape on Molecular Taper Angle. *Chem. - Eur. J.* **2000**, *6*, 1258−1266.

(32) Percec, V.; Peterca, M.; Dulcey, A. E.; Imam, M. R.; Hudson, S. D.; Nummelin, S.; Adelman, P.; Heiney, P. A. Hollow Spherical Supramolecular Dendrimers. *J. Am. Chem. Soc.* **2008**, *130*, 13079−13094.

(33) Ungar, G.; Liu, Y.; Zeng, X.; Percec, V.; Cho, W.-D. Giant Supramolecular Liquid Crystal Lattice. *Science* **2003**, *299*, 1208−1211.

https://dx.doi.org/10.1021/acsanm.0c00231
ACS Appl. Nano Mater. 2020, 3, 2952−2958

(34) Zeng, X.; Ungar, G.; Liu, Y.; Percec, V.; Dulcey, A. E.; Hobbs, J. K. Supramolecular dendritic liquid quasicrystals. *Nature* **2004**, *428*, 157−160.
(35) Ungar, G.; Percec, V.; Zeng, X.; Leowanawat, P. Liquid Quasicrystals. *Isr. J. Chem.* **2011**, *51*, 1206−1215.
(36) Tomalia, D. A.; Khanna, S. N. A Systematic Framework and Nanoperiodic Concept for Unifying Nanoscience: Hard/Soft Nanoelements, Superatoms, Meta-Atoms, New Emerging Properties, Periodic Property Patterns, and Predictive Mendeleev-like Nanoperiodic Tables. *Chem. Rev.* **2016**, *116*, 2705−2774.
(37) Li, Y.; Lin, S.-T.; Goddard, W. A. Efficiency of Various Lattices from Hard Ball to Soft Ball: Theoretical Study of Thermodynamic Properties of Dendrimer Liquid Crystal from Atomistic Simulation. *J. Am. Chem. Soc.* **2004**, *126*, 1872−1885.
(38) Iacovella, C. R.; Keys, A. S.; Glotzer, S. C. Self-assembly of soft-matter quasicrystals and their approximants. *Proc. Natl. Acad. Sci. U. S. A.* **2011**, *108*, 20935−20940.
(39) Ye, X.; Chen, J.; Eric Irrgang, M.; Engel, M.; Dong, A.; Glotzer, S. C.; Murray, C. B. Quasicrystalline nanocrystal superlattice with partial matching rules. *Nat. Mater.* **2017**, *16*, 214−219.
(40) Wan, D.; Du, C. X.; van Anders, G.; Glotzer, S. C. FCC ↔ BCC Phase Transitions in Convex and Concave Hard Particle Systems. *J. Phys. Chem. B* **2019**, *123*, 9038−9043.
(41) Ziherl, P.; Kamien, R. D. Soap Froths and Crystal Structures. *Phys. Rev. Lett.* **2000**, *85*, 3528−3531.
(42) Ziherl, P.; Kamien, R. D. Maximizing Entropy by Minimizing Area: Towards a New Principle of Self-Organization. *J. Phys. Chem. B* **2001**, *105*, 10147−10158.
(43) Grason, G. M. The packing of soft materials: Molecular asymmetry, geometric frustration and optimal lattices in block copolymer melts. *Phys. Rep.* **2006**, *433*, 1−64.
(44) Xie, N.; Li, W.; Qiu, F.; Shi, A.-C. σ Phase Formed in Conformationally Asymmetric AB-Type Block Copolymers. *ACS Macro Lett.* **2014**, *3*, 906−910.
(45) Li, W.; Duan, C.; Shi, A.-C. Nonclassical Spherical Packing Phases Self-Assembled from AB-Type Block Copolymers. *ACS Macro Lett.* **2017**, *6*, 1257−1262.
(46) Bates, M. W.; Lequieu, J.; Barbon, S. M.; Lewis, R. M.; Delaney, K. T.; Anastasaki, A.; Hawker, C. J.; Fredrickson, G. H.; Bates, C. M. Stability of the A15 phase in diblock copolymer melts. *Proc. Natl. Acad. Sci. U. S. A.* **2019**, *116*, 13194−13199.
(47) Zhang, W.-B.; Yu, X.; Wang, C.-L.; Sun, H.-J.; Hsieh, I. F.; Li, Y.; Dong, X.-H.; Yue, K.; Van Horn, R.; Cheng, S. Z. D. Molecular Nanoparticles Are Unique Elements for Macromolecular Science: From "Nanoatoms" to Giant Molecules. *Macromolecules* **2014**, *47*, 1221−1239.
(48) Liu, H.; Luo, J.; Shan, W.; Guo, D.; Wang, J.; Hsu, C.-H.; Huang, M.; Zhang, W.; Lotz, B.; Zhang, W.-B.; Liu, T.; Yue, K.; Cheng, S. Z. D. Manipulation of Self-Assembled Nanostructure Dimensions in Molecular Janus Particles. *ACS Nano* **2016**, *10*, 6585−6596.
(49) Zhang, W.; Liu, Y.; Huang, J.; Liu, T.; Xu, W.; Cheng, S. Z. D.; Dong, X.-H. Engineering self-assembly of giant molecules in the condensed state based on molecular nanoparticles. *Soft Matter* **2019**, *15*, 7108−7116.
(50) Hsu, C.-H.; Dong, X.-H.; Lin, Z.; Ni, B.; Lu, P.; Jiang, Z.; Tian, D.; Shi, A.-C.; Thomas, E. L.; Cheng, S. Z. D. Tunable Affinity and Molecular Architecture Lead to Diverse Self-Assembled Supramolecular Structures in Thin Films. *ACS Nano* **2016**, *10*, 919−929.
(51) Zhang, W.; Chu, Y.; Mu, G.; Eghtesadi, S. A.; Liu, Y.; Zhou, Z.; Lu, X.; Kashfipour, M. A.; Lillard, R. S.; Yue, K.; Liu, T.; Cheng, S. Z. D. Rationally Controlling the Self-Assembly Behavior of Triarmed POSS−Organic Hybrid Macromolecules: From Giant Surfactants to Macroions. *Macromolecules* **2017**, *50*, 5042−5050.
(52) Zhang, W.; Huang, M.; Su, H.; Zhang, S.; Yue, K.; Dong, X.-H.; Li, X.; Liu, H.; Zhang, S.; Wesdemiotis, C.; Lotz, B.; Zhang, W.-B.; Li, Y.; Cheng, S. Z. D. Toward Controlled Hierarchical Heterogeneities in Giant Molecules with Precisely Arranged Nano Building Blocks. *ACS Cent. Sci.* **2016**, *2*, 48−54.
(53) Zhang, W.; Lu, X.; Mao, J.; Hsu, C.-H.; Mu, G.; Huang, M.; Guo, Q.; Liu, H.; Wesdemiotis, C.; Li, T.; Zhang, W.-B.; Li, Y.; Cheng, S. Z. D. Sequence-Mandated, Distinct Assembly of Giant Molecules. *Angew. Chem., Int. Ed.* **2017**, *56*, 15014−15019.
(54) Zhang, W.; Zhang, S.; Guo, Q.; Lu, X.; Liu, Y.; Mao, J.; Wesdemiotis, C.; Li, T.; Li, Y.; Cheng, S. Z. D. Multilevel Manipulation of Supramolecular Structures of Giant Molecules via Macromolecular Composition and Sequence. *ACS Macro Lett.* **2018**, *7*, 635−640.
(55) García, F.; Viruela, P. M.; Matesanz, E.; Ortí, E.; Sánchez, L. Cooperative Supramolecular Polymerization and Amplification of Chirality in C3-Symmetrical OPE-Based Trisamides. *Chem. - Eur. J.* **2011**, *17*, 7755−7759.
(56) Wang, F.; Gillissen, M. A. J.; Stals, P. J. M.; Palmans, A. R. A.; Meijer, E. W. Hydrogen Bonding Directed Supramolecular Polymerisation of Oligo(Phenylene-Ethynylene)s: Cooperative Mechanism, Core Symmetry Effect and Chiral Amplification. *Chem. - Eur. J.* **2012**, *18*, 11761−11770.
(57) Park, S.; Cho, B.-K. Sequential phase transformation of propeller-like C3-symmetric liquid crystals from a helical to ordered to disordered hexagonal columnar structure. *Soft Matter* **2015**, *11*, 94−101.
(58) Percec, V.; Cho, W.-D.; Ungar, G. Increasing the Diameter of Cylindrical and Spherical Supramolecular Dendrimers by Decreasing the Solid Angle of Their Monodendrons via Periphery Functionalization. *J. Am. Chem. Soc.* **2000**, *122*, 10273−10281.
(59) Percec, V.; Imam, M. R.; Peterca, M.; Wilson, D. A.; Heiney, P. A. Self-Assembly of Dendritic Crowns into Chiral Supramolecular Spheres. *J. Am. Chem. Soc.* **2009**, *131*, 1294−1304.
(60) Percec, V.; Imam, M. R.; Peterca, M.; Wilson, D. A.; Graf, R.; Spiess, H. W.; Balagurusamy, V. S. K.; Heiney, P. A. Self-Assembly of Dendronized Triphenylenes into Helical Pyramidal Columns and Chiral Spheres. *J. Am. Chem. Soc.* **2009**, *131*, 7662−7677.
(61) Sahoo, D.; Peterca, M.; Aqad, E.; Partridge, B. E.; Heiney, P. A.; Graf, R.; Spiess, H. W.; Zeng, X.; Percec, V. Hierarchical Self-Organization of Perylene Bisimides into Supramolecular Spheres and Periodic Arrays Thereof. *J. Am. Chem. Soc.* **2016**, *138*, 14798−14807.
(62) Sahoo, D.; Peterca, M.; Aqad, E.; Partridge, B. E.; Heiney, P. A.; Graf, R.; Spiess, H. W.; Zeng, X.; Percec, V. Tetrahedral Arrangements of Perylene Bisimide Columns via Supramolecular Orientational Memory. *ACS Nano* **2017**, *11*, 983−991.
(63) Frigo, M.; Johnson, S. G. The Design and Implementation of FFTW3. *Proc. IEEE* **2005**, *93*, 216−231.
(64) Percec, V.; Peterca, M.; Tsuda, Y.; Rosen, B. M.; Uchida, S.; Imam, M. R.; Ungar, G.; Heiney, P. A. Elucidating the Structure of the $Pm\bar{3}n$ Cubic Phase of Supramolecular Dendrimers through the Modification of their Aliphatic to Aromatic Volume Ratio. *Chem. - Eur. J.* **2009**, *15*, 8994−9004.
(65) Peterca, M.; Imam, M. R.; Leowanawat, P.; Rosen, B. M.; Wilson, D. A.; Wilson, C. J.; Zeng, X.; Ungar, G.; Heiney, P. A.; Percec, V. Self-Assembly of Hybrid Dendrons into Doubly Segregated Supramolecular Polyhedral Columns and Vesicles. *J. Am. Chem. Soc.* **2010**, *132*, 11288−11305.
(66) Weaire, D.; Phelan, R. A counter-example to Kelvin's conjecture on minimal surfaces. *Philos. Mag. Lett.* **1994**, *69*, 107−110.
(67) Travesset, A. Nanoparticle Superlattices as Quasi-Frank-Kasper Phases. *Phys. Rev. Lett.* **2017**, *119*, 115701.
(68) Girard, M.; Wang, S.; Du, J. S.; Das, A.; Huang, Z.; Dravid, V. P.; Lee, B.; Mirkin, C. A.; Olvera de la Cruz, M. Particle analogs of electrons in colloidal crystals. *Science* **2019**, *364*, 1174−1178.
(69) Peterca, M.; Imam, M. R.; Hudson, S. D.; Partridge, B. E.; Sahoo, D.; Heiney, P. A.; Klein, M. L.; Percec, V. Complex Arrangement of Orthogonal Nanoscale Columns via a Supramolecular Orientational Memory Effect. *ACS Nano* **2016**, *10*, 10480−10488.
(70) Sahoo, D.; Imam, M. R.; Peterca, M.; Partridge, B. E.; Wilson, D. A.; Zeng, X.; Ungar, G.; Heiney, P. A.; Percec, V. Hierarchical Self-Organization of Chiral Columns from Chiral Supramolecular Spheres. *J. Am. Chem. Soc.* **2018**, *140*, 13478−13487.

https://dx.doi.org/10.1021/acsanm.0c00231
ACS Appl. Nano Mater. 2020, 3, 2952−2958